Angewandte Chemie
Eine Zeitschrift der Gesellschaft Deutscher Chemiker

Supporting Information

A Supramolecular Crosslinker to Give Salt-Resistant Polyion Complex Micelles and Improved MRI Contrast Agents

Jiahua Wang, Junyou Wang, Peng Ding, Wenjuan Zhou, Yuehua Li, Markus Drechsler, Xuhong Guo,* and Martien A. Cohen Stuart**

anie_201805707_sm_miscellaneous_information.pdf

SUPPORTING INFORMATION

Table of Contents

Experimental Section

Materials

The diblock copolymer, poly(N-methyl-2-vinyl-pyridinium iodide)-*b*-poly(ethyleneoxide) ($P2MVP_{41}$-*b*-PEO_{205}), was obtained by quaternization of poly(2-vinylpyridine)-*b*-poly(ethylene oxide) ($P2VP_{41}$-*b*-PEO_{205}) (Polymer Source, Mw/Mn= 1.03, Mw= 13.3 k) following a procedure described elsewhere.[1] The degree of quaternization is about 90%. The bis-ligand compound 1,11-bis(2,6-dicarboxypyridin-4-yloxy)-3,6,9-trioxaundecane (L_2) was prepared according to literature. [2] 4-hydroxypyridine-2,6-dicarboxylic acid (chelidamic acid), Iron(III) chloride hexahydrate $FeCl_3 \cdot 6H_2O$, Manganese(II) nitrate tetrahydrate $Mn(NO_3)_2 \cdot 4H_2O$ and sodium chloride $NaNO_3$ (analytical grade) were purchased from Sigma Aldrich and used without further purification. Fe-L_3/L_2 micelles solutions were made in acetate buffer at pH 5 and Mn-L_3/L_2 micelles solutions were made in tris(hydroxymethyl)aminomethane (Tris) buffer at pH 7.4.

Characterizations

^{1}H-NMR spectra and ^{13}C-NMR spectra were recorded on a BRUKER AVANCE 500 spectrometer operating at 500 MHz. UV spectra for all the samples were recorded on an SHIMADZU 1800 spectrophotometer. The MRI testing and T_1 relaxation time measurements were tested at a 0.47 T NMRI20-Analyst NMR Analyzing and Imaging system (Niumag Corporation, Shanghai, China).

Synthesis of 1,3,5-tris(2,6-dicarboxypyridin-4-yloxymethyl)benzene, L_3.

4-hydroxypyridine-2,6-dicarboxylic acid (chelidamic acid) **1** (2.5g, 13.3mmol) was added to a solution of thionyl chloride (7.5ml) in ethanol (25ml) at -10 °C. The mixture was stirred at room temperature for 24 h and then refluxed for an additional 2 h. After cooling, the mixture was concentrated under reduced pressure to give a residue, which was treated with water (20ml). The resultant suspension, cooled to 0 °C, was neutralized with 10% aq. Na_2CO_3, and filtered. The solid material was dried and recrystallized from ethanol-water (1:2) and dried under reduced pressure at 50 °C to give the diethylester **2** as white crystals. [3] A mixture of compound $_2$ (2.5g, 10.45mmol) and anhydrous potassium carbonate (1.31g, 9.5mmol) in dry N,N-dimethyformamide (40ml) was stirred at 25 °C in vacuo for 30 minutes, then 1,3,5-tirs(bromomethyl)benzene **3** (1.13g, 3.17mmol) was added and the reaction mixture was allowed to react at 70-80 °C for 24 hours under an atmosphere of argon. The mixture was evaporated in vacuo and the residue was partitioned between dichloromethane and water. The organic layer was washed with 1% aqueous acetic acid, water and dried (sodium sulfate). The residue obtained, after removal of the solvent, was recrystallized from ethanol and dried in vacuo at 50 °C to give **4** as a white solid. [4] Hydrolysis of 2.8 g of this ester was performed by heating it in a mixture of 30 ml deionized water, 30 ml ethanol and KOH (3.37g, 60mmol) for 12 h at 60 ºC. The product could be precipitated in a mixture of ethanol and water. The precipitate was washed with ice water and ethanol and freeze-dried to give the desired product **5**. Yield: 57% (2.3 g, 2.58 mmol), mp > 300 ºC. ^{1}H NMR (D_2O): δ 5.30 (s, 6H, CH_2), 7.59 (s, 6H, aromatic H), 7.66 (s, 3H, aromatic H). ^{13}C NMR (D2O): δ 69.74 (CH_2), 111.50 (CH), 127.51 (CH), 136.73 (C), 154.83 (C), 166.30 (CO), 172.56 (CO_2).

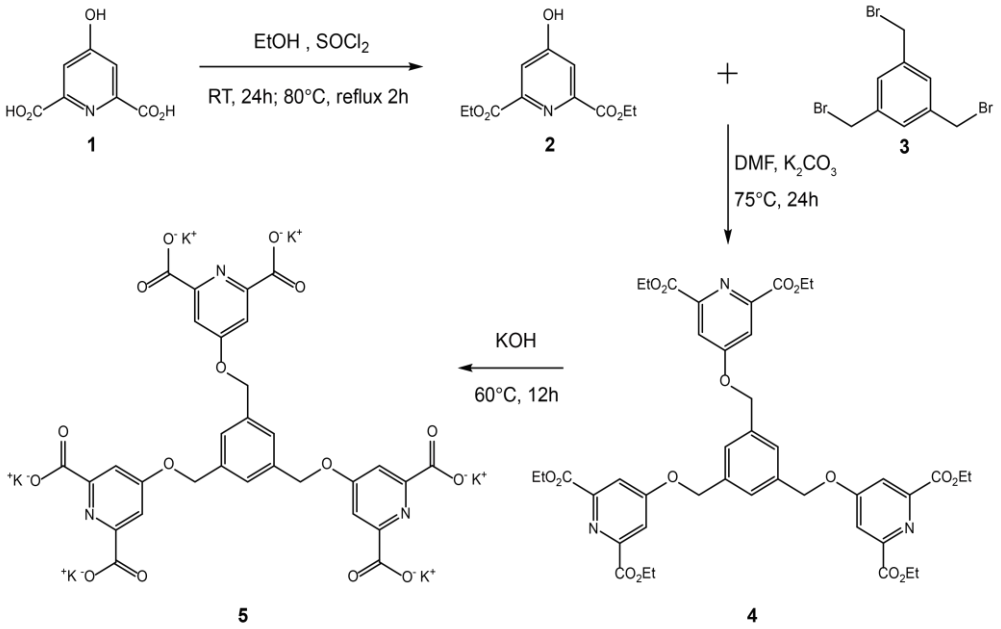

Scheme SI 1. Synthesis of L_3 ligand.

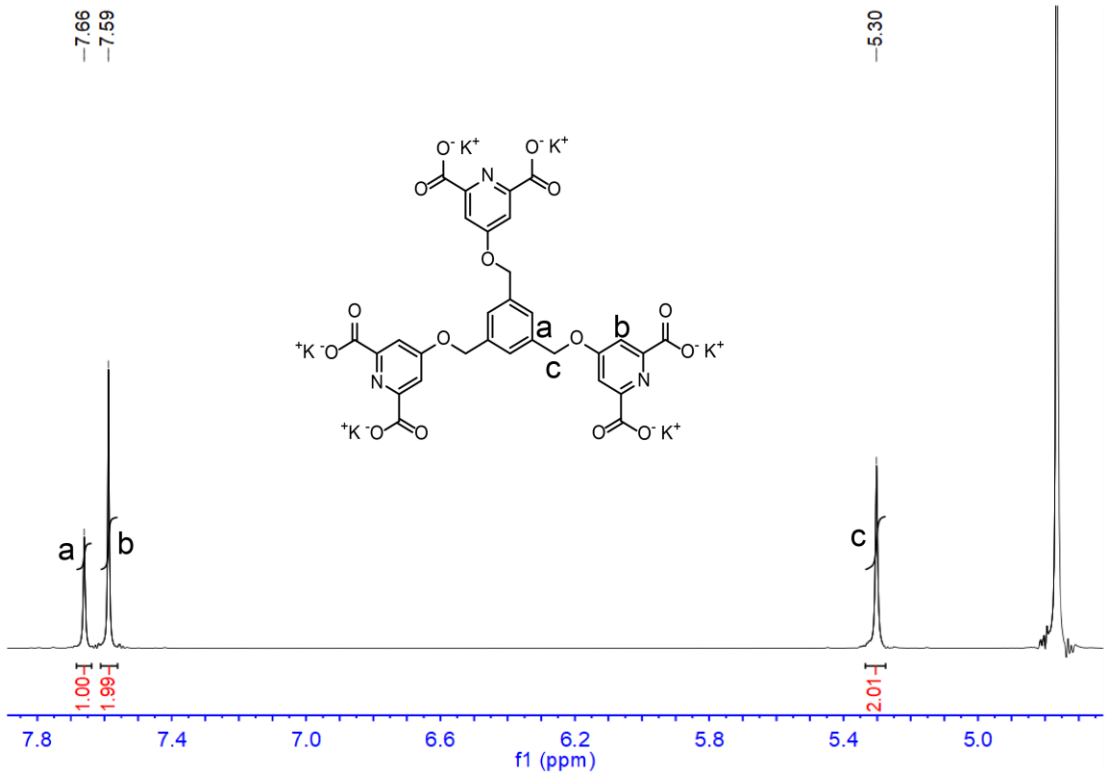

Figure SI 1. ^{1}H-NMR spectrum of the tris-ligand L_3. L_3 was dissolved in D_2O and measured at 298 K on BRUKER AVANCE III 500 spectrometer (500 MHz).

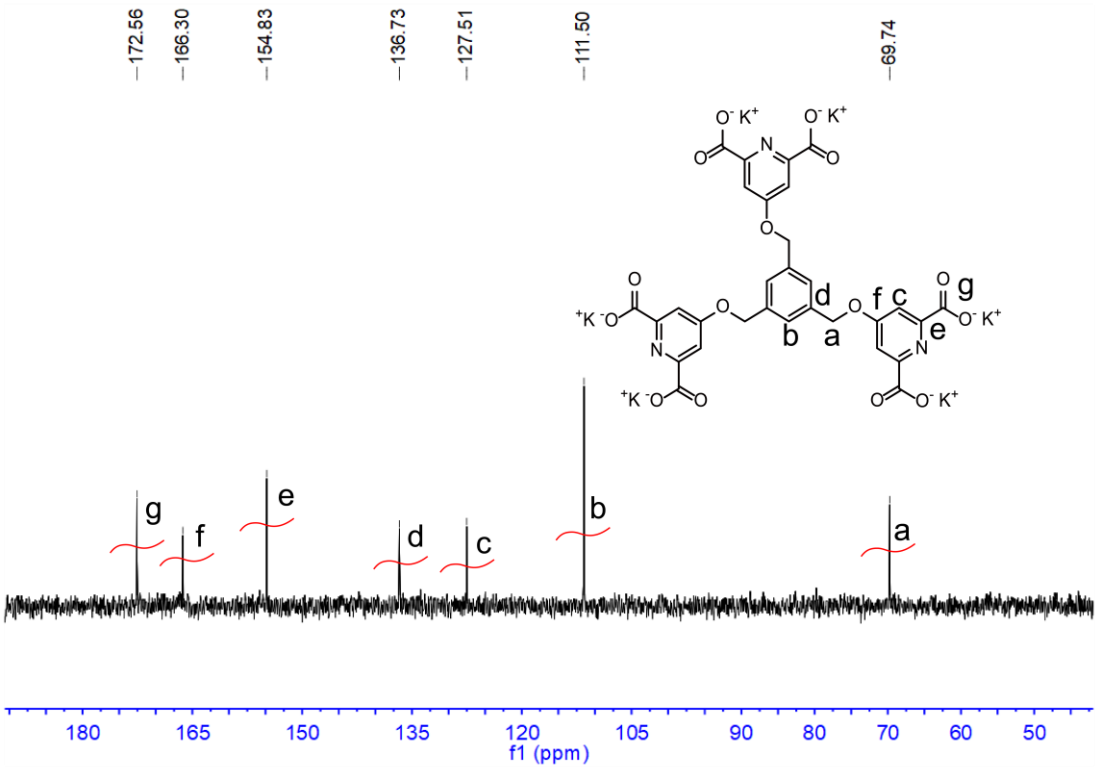

Figure SI 2. ^{13}C-NMR spectrum of the tris-ligand L_3.

Preparing micelles – experimental protocol

Micellar solutions were prepared by first mixing the diblock copolymer with the ligands at the relevant salt concentration. Then, a solution of the transition metal (as nitrate) was added under stirring.

Light Scattering

The Dynamic light scattering (DLS) measurement was performed with an ALV light scattering apparatus, equipped with a 400 mW argon ion laser operating at a wavelength of 532 nm. Measurements were done at a detection angle of 90°, unless stated otherwise. All measurements were performed at room temperature.

The light scattering intensity is expressed as the excess Rayleigh ratio R_θ divided by the polymer concentration. R_θ is obtained as (1) where I_{sample} is the scattering intensity of the complex solution and $I_{solvent}$ is the intensity of the solvent. $I_{toluene}$ is the scattering intensity of toluene (the reference), and $R_{toluene}$ is the known Rayleigh ratio of toluene (2.1×10^{-2} m^{-1}).

$$R_\theta = \frac{I_{sample} - I_{solvent}}{I_{toluene}} \times R_{tuluene} \times \frac{n^2_{solvent}}{n^2_{toluene}} \qquad (1)$$

Salt stability of the micelles was tested by titrating concentrated $NaNO_3$ solution into the micelles solution. The scattering intensity and hydrodynamic radius was recorded for each titration step.

The CUMULANT method was used to analyze the mean apparent hydrodynamic radius (R_h), which is

$$R_h=kTq^2/6\pi\eta\Gamma \quad (2)$$

where q is the scattering vector, k is the Boltzmann constant, T is the absolute temperature, η is the viscosity of the solvent, and Γ is the measured average decay rate of the correlation function. The CONTIN method is used to analyze the distribution of particle (C3Ms) radius.

For angular-dependent DLS, ten correlation functions $g_2(t)$ were recorded at 6 angles θ, from 60 to 135° in increments of 15°, to evaluate the angular dependence of the diffusion coefficient. It is known that asymmetric particles always give rise to a dependence of D (= Γ/q^2) on q^2, but for spherical particles, the D (= Γ/q^2) values should be independent of the scattering vector, because of the undetectable rotational motion. [5] where q is the scattering vector:

$$q=(4\pi n/\lambda)\sin(\theta/2) \quad (3)$$

Cryogenic Transmission Electronic Microscopy (Cryo-TEM)

A few microliters of samples were placed on a bare copper TEM grid (Plano, 600 mesh), and the excess liquid was removed with filter paper. This sample was cryo-fixed by rapidly immersing into liquid ethane cooled to -170 to -180 °C in a cryo-box (Carl Zeiss NTS GmbH). The specimen was inserted into a cryo-transfer holder (CT3500, Gatan, Munich, Germany) and transferred to a Zeiss EM922 EFTEM (Zeiss NTS GmbH, Oberkochen, Germany). Examinations were carried out at temperatures around -180 °C. The TEM was operated at an acceleration voltage of 200 kV. Zero-loss filtered images were taken under reduced dose conditions (500-2000 e/nm^2). All images were recorded digitally by a bottom-mounted CCD camera system (UltraScan 1000, Gatan) and processed with a digital imaging processing system (Digital Micrograph 3.9 for GMS 1.4, Gatan).

Cytotoxicity Assay

Cell viability was determined by a typical 3-(4,5-dimethyl-2-yl)-2,5-diphenyltetrazolium bromide (MTT) assay. SMCC-7721 cells were seeded into a 96-well culture plate at a density of 5 × 103 cells well^{-1} and cultured for 24 h in a 5% CO_2 incubator at 37 °C. The cells were treated with Mn-L_3 micelles at 0–60 μM or vehicle control for 24 h; the cell viability was measured by a microplate reader at 490 nm with the MTT staining assay. Optical density (OD) was read at 490 nm and background was subtracted at 630 nm using a spectrophotometer (SpectraMax M2, Molecular Devices, USA). Cell viability was expressed as a percentage of the corresponding control value. The data are expressed as the average of five replicates ± standard deviations (SD).

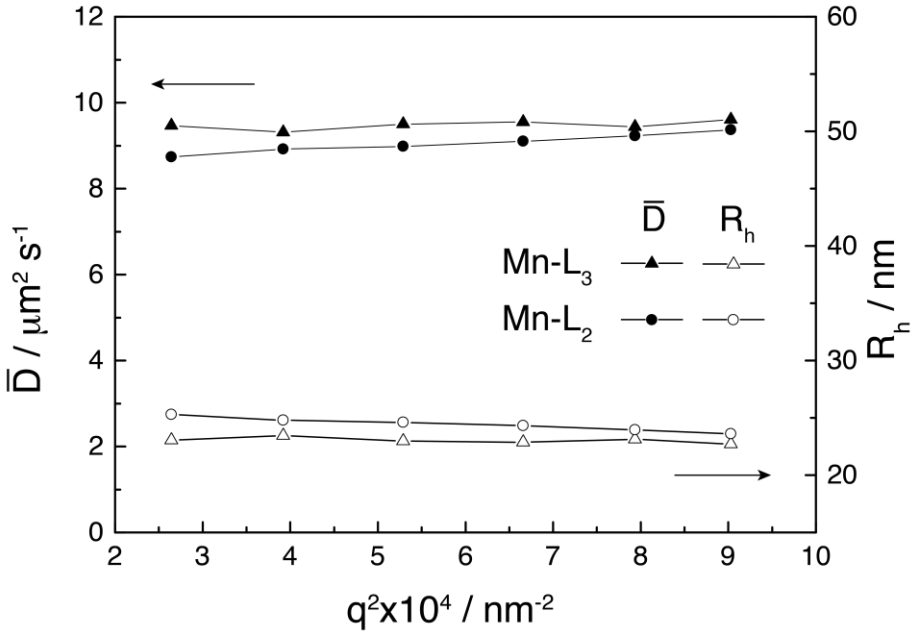

Figure SI 3. Angular dependence of the apparent particle radius (solid) and the self-diffusion coefficient (open) for Mn-L_2 and Mn-L_3 micelles systems.

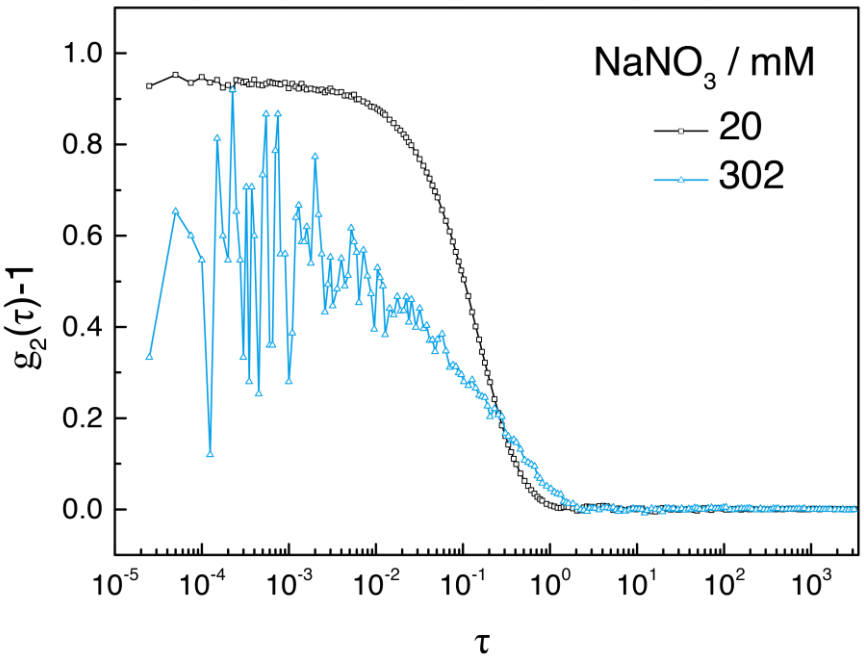

Figure SI 4. The autocorrelation function for Mn-L_2 micelles (0% of L_3) at low and high salt concentration.

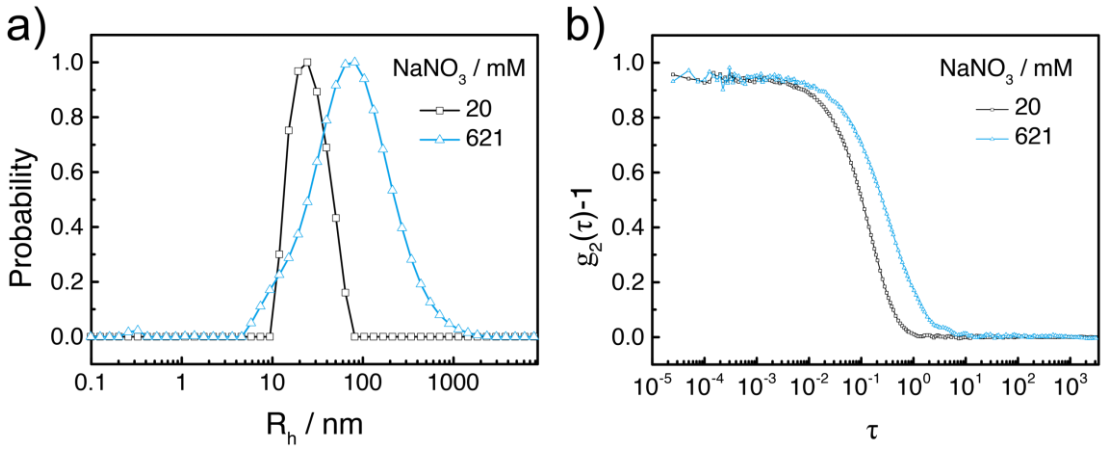

Figure SI 5. a: size and size distribution of Mn-L_2-L_3 micelles (20% of L_3) at low and high salt concentration; b: the autocorrelation function for Mn-L_2-L_3 micelles at low and high salt concentration.

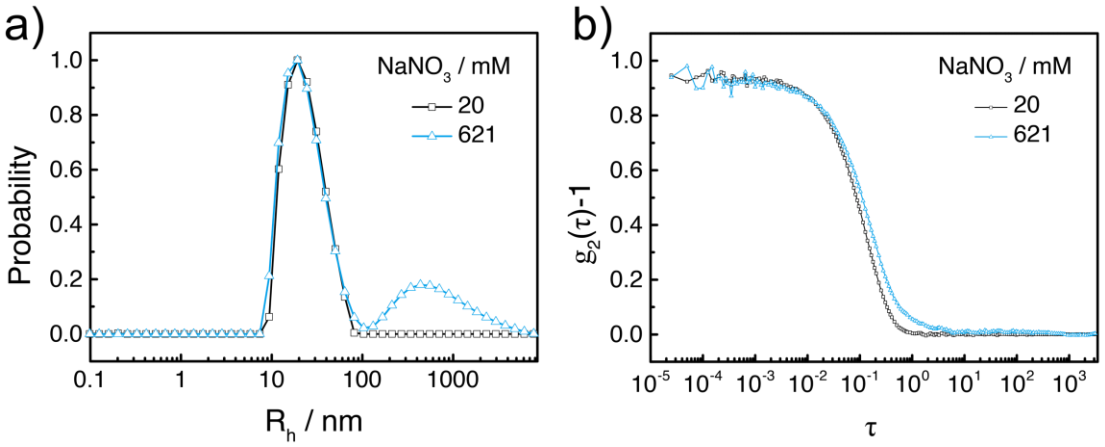

Figure SI 6. a: size and size distribution of Mn-L_2-L_3 micelles (40% of L_3) at low and high salt concentration; b: the autocorrelation function for Mn-L_2-L_3 micelles at low and high salt concentration.

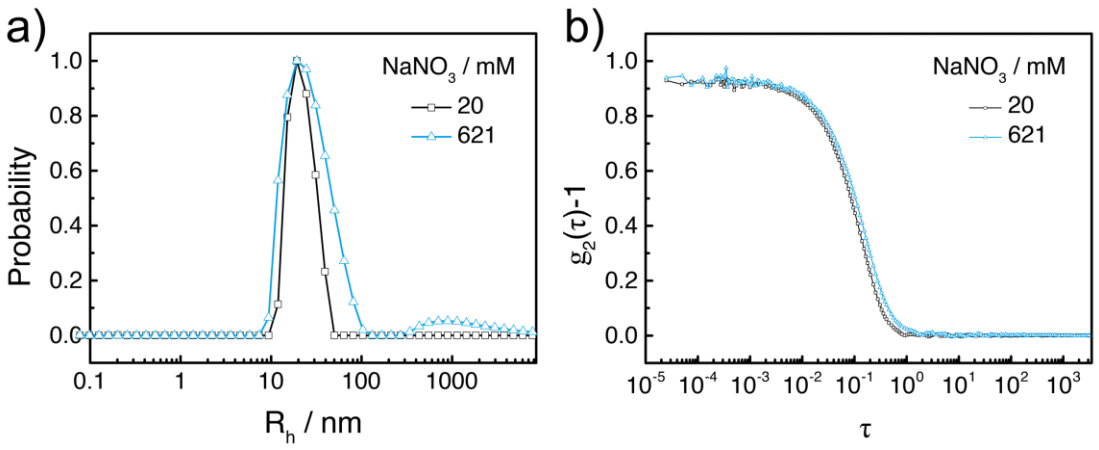

Figure SI 7. a: size and size distribution of Mn-L_2-L_3 micelles (60% of L_3) at low and high salt concentration; b: the autocorrelation function for Mn-L_2-L_3 micelles at low and high salt concentration.

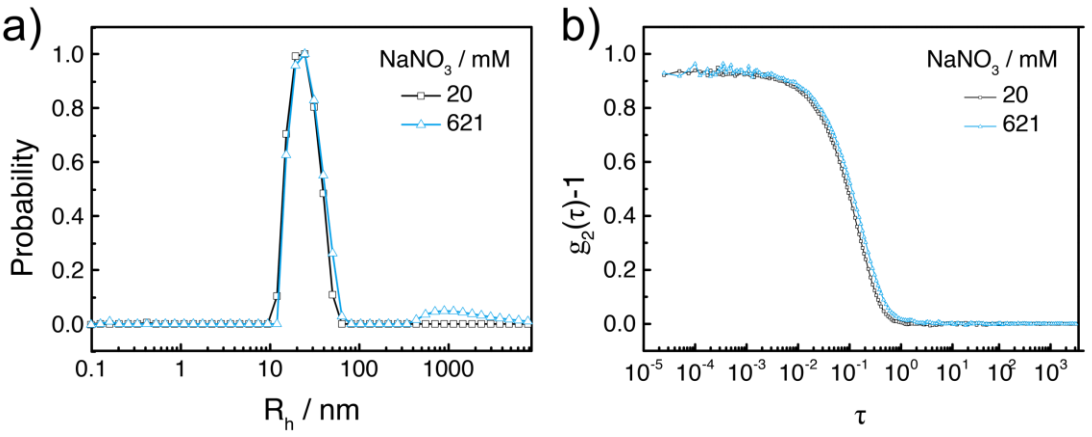

Figure SI 8. a: size and size distribution of Mn-L_2-L_3 micelles (80% of L_3) at low and high salt concentration; b: the autocorrelation function for Mn-L_2-L_3 micelles at low and high salt concentration.

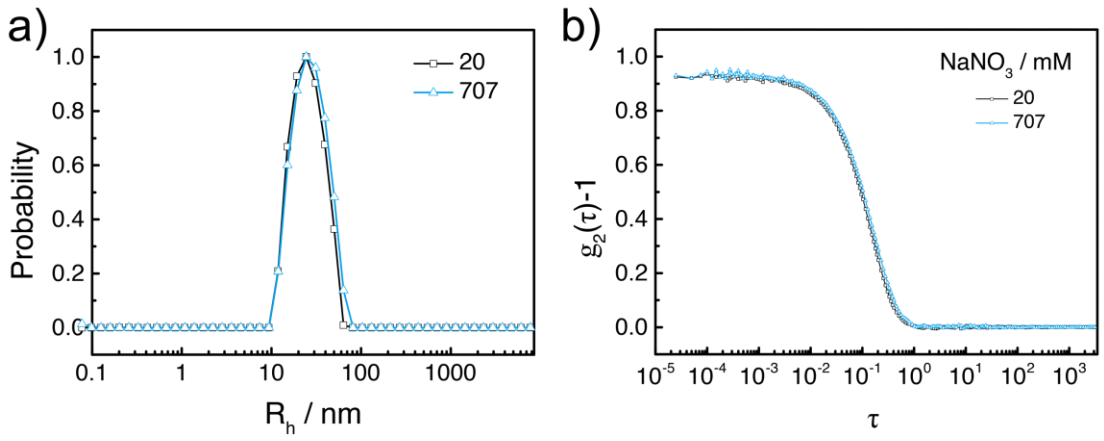

Figure SI 9. a: size and size distribution of Mn-L_3 micelles (100% of L_3) at low and high salt concentration; b: the autocorrelation function for Mn-L_2-L_3 micelles at low and high salt concentration.

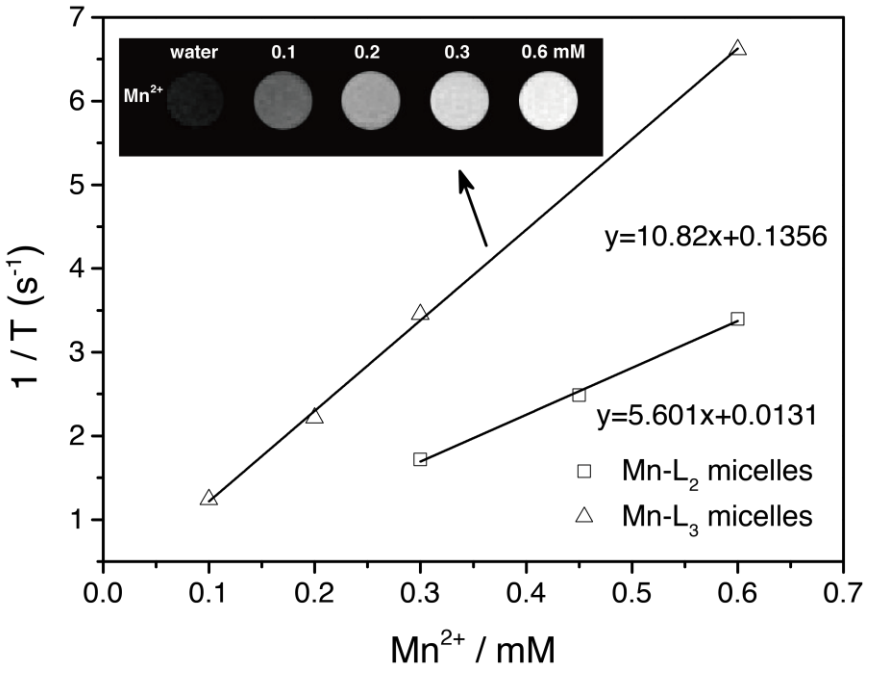

Figure SI 10. Plots of longitudinal relaxation rate, $1/T_1$ vs Mn^{2+} concentration for Mn-L_2 micelles and Mn-L_3 micelles solutions, inset figure is vitro T_1-weighted MR imaging of Mn-L_3 micelles at various Mn^{2+} concentration.

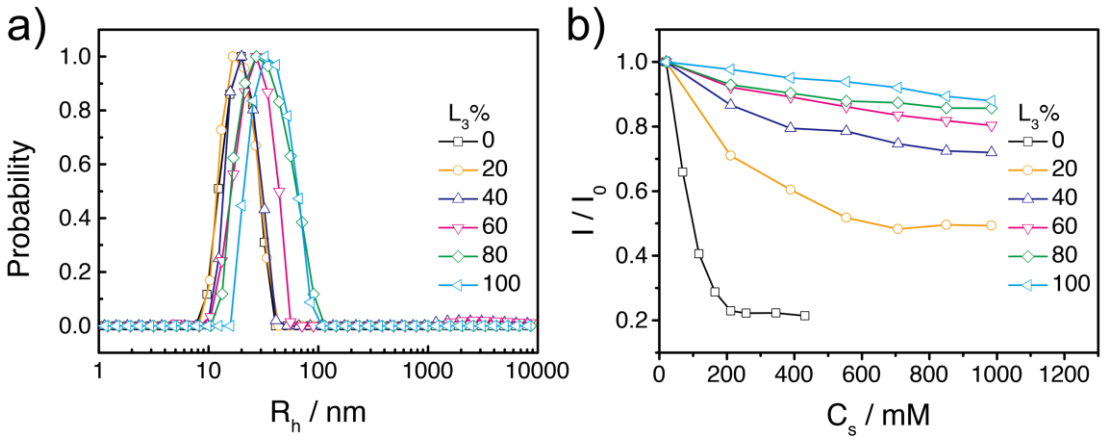

Figure SI 11. a: size and size distribution of Fe-L_2-L_3 micelles as a function of L_3 ligand percentage; b: Scattering intensity (normalized by the original value I_0, where no salt is added yet) for Fe-L_2-L_3 micelles at different L_3% with increasing salt concentration.

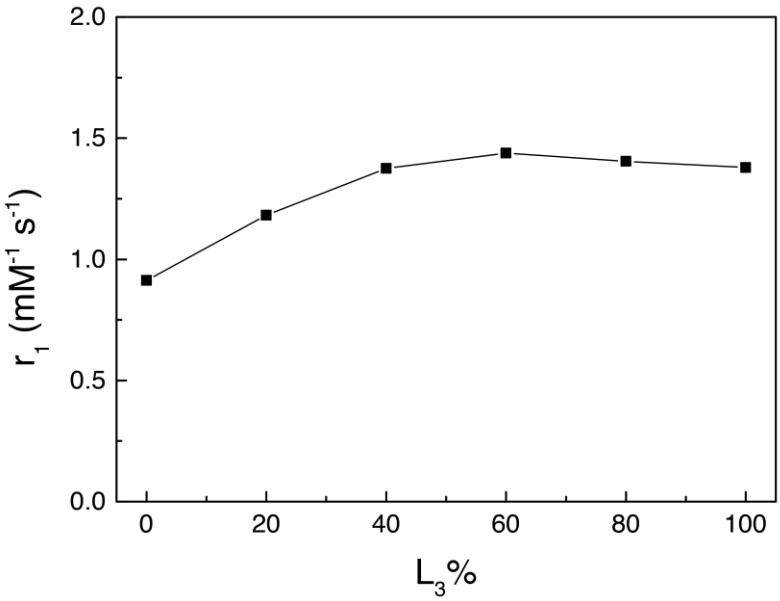

Figure SI 12. The relaxivity r_1 of Fe-L_2-L_3 micelles at different L_3 fractions. r_1 is the longitudinal relaxivity of water protons in the presence of Fe-L_2-L_3 micelles.

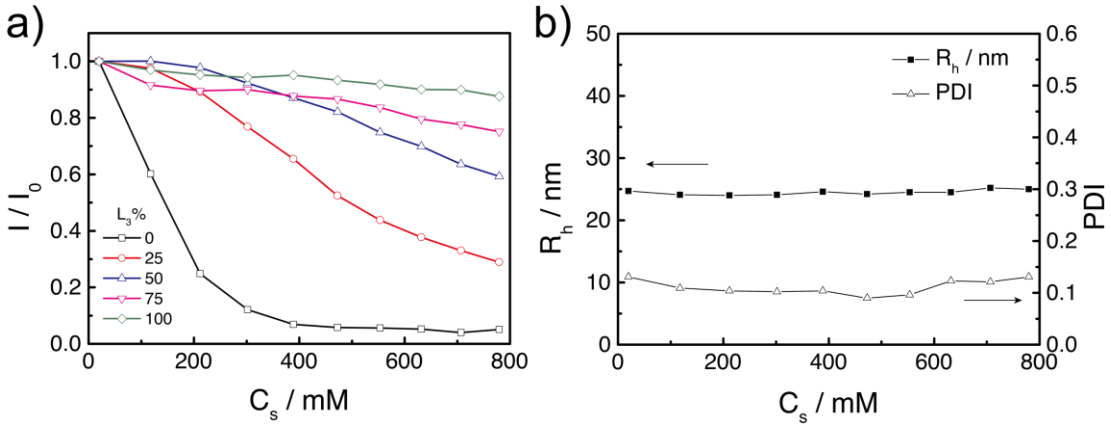

Figure SI 13. a: Scattering intensity of Zn-L_2-L_3 micelles at different L_3% with increasing salt concentration; b: R_h and PDI of Zn(II)-L_3 micelles.

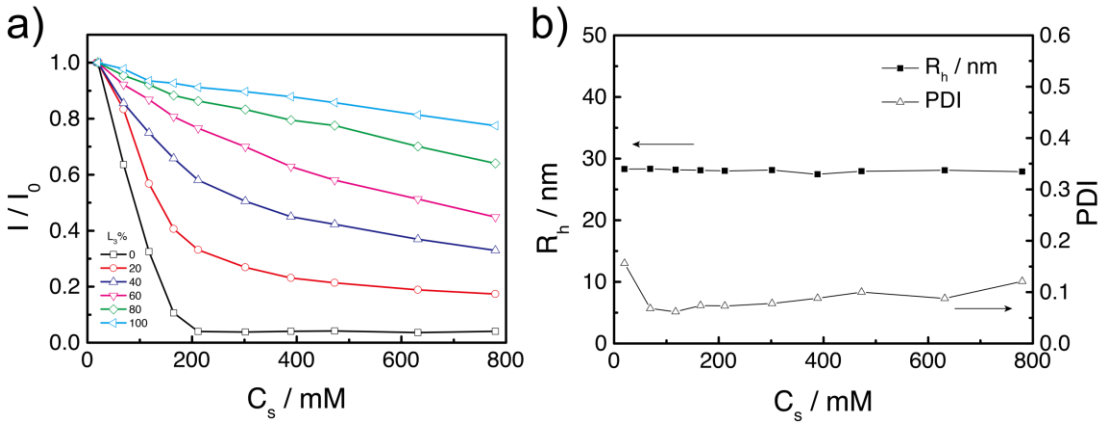

Figure SI 14. a: Scattering intensity for Ni-L_2-L_3 micelles at different L_3% with increasing salt concentration; b: R_h and PDI of Ni-L_3 micelles.

References

[1] M. Biesalski, D. Johannsmann, J. Ruhe, *J. Chem. Phys.* **2004**, *120*, 8807-8814.

[2] T. Vermonden, D. Branowska, A. T. M Marcelis, E. J. R. Sudholter, *Tetrahedron* **2003**, *59*, 5039-5045.

[3] G. Chessa, A, Scrivanti, *J. Chem. Soc., Perkin Trans. 1* **1996**, 307–311.

[4] G. Chessa, A, Scrivanti, *J. Heterocyclic Chem.* **1997**, *34*, 1851-1855.

[5] Yun Yan, Nicolaas A.M. Besseling, Arie de Keizer, Markus Drechsler, Remco Fokkink, and Martien A. Cohen Stuart, *J. Phys. Chem. B* **2007,** *111,* 11662-11669